Packing fraction of particles with lognormal size distribution

H. J. H. Brouwers
Department of the Built Environment, Eindhoven University of Technology, P. O. Box 513, 5600 MB Eindhoven, The Netherlands
(Received 1 January 2014; published 21 May 2014)

This paper addresses the packing and void fraction of polydisperse particles with a lognormal size distribution. It is demonstrated that a binomial particle size distribution can be transformed into a continuous particle-size distribution of the lognormal type. Furthermore, an original and exact expression is derived that predicts the packing fraction of mixtures of particles with a lognormal distribution, which is governed by the standard deviation, mode of packing, and particle shape only. For a number of particle shapes and their packing modes (close, loose) the applicable values are given. This closed-form analytical expression governing the packing fraction is thoroughly compared with empirical and computational data reported in the literature, and good agreement is found.

DOI: 10.1103/PhysRevE.89.052211 PACS number(s): 45.70.Cc, 81.05.Rm, 71.55.Jv

I. INTRODUCTION

Lognormal (or log-normal) distributions are widespread in the physical, biological, social, and economic sciences [1–4]. Particles that result from natural weathering or industrial comminution [5], or are formed by condensation or solidification processes [6,7], often closely fit the lognormal distribution. The packing of particles is relevant to physicists, biologists, and engineers. There is practical as well as fundamental interest in understanding the relationship between the particle shape and particle-size distribution, on the one hand, and the packing fraction, on the other.

The packing fraction of particles depends on their shape and method of packing, ordered or disordered (random), where the latter furthermore depends on the densification. In nature and technology, often a wide variety of randomlike packings are found, also referred to as jammed or disordered packings. Examples are packings of rice grains, cement, sand, medical powders, ceramic powders, fibers, and atoms in amorphous materials. Particles possess a monosized packing fraction that depends on the particle shape and the method of packing [random loose packing (RLP) or random close packing (RCP)]. For RCP of uniform spheres the packing fraction (f_1) was experimentally found to be 0.64 [8], being in line with computer-generated values [9–14]. Also for RLP of monosized spheres a reproducible packing fraction is found [8,15–18], with $f_1^{\mathrm{rlp}} \approx 0.54$ as a generally accepted value for this lower limit of random sphere packings. For a number of nonspherical, but regular, particle (grain) shapes the monosized packing fraction has been computed and or measured for disks [19], thin rods [20], and ellipsoids [21]. For irregularly shaped particles much work has been done on the prediction of the unimodal void fraction using shape factors, etc., but for many irregular shapes it is still recommendable to obtain the monosized void fraction from experiments.

Another complication arises when particles or atoms of different sizes are randomly packed, which is often the case for products processed from granular materials and in amorphous alloys. For discrete and continuous geometric packings closed-form solutions have been presented [22–24]. For continuous normal and lognormal distributions of sands, Sohn and Moreland [25] determined experimentally the packing fraction as a function of the standard deviation. For discrete lognormal distributions of steel spheres Dexter and Tanner [26] measured the packing fraction as function of the standard deviation. Yang *et al.* [11] and He *et al.* [12] reported computational simulations of sphere packings. In this paper, a closed-form equation is derived for the packing fraction of particles with lognormal size distribution.

To this end, in Sec. II the theory of Furnas [27] on binary mixes with large size ratio, i.e., two noninteracting fractions, is recapitulated. Whereas Furnas addressed saturated packings, i.e., packings where the composition is such that the small fractions fits in the voids of the larger fraction, here the packing fraction in the entire compositional range is addressed. Subsequently, this model is applied to the case of a ternary mix of noninteracting fractions, whereby the three fractions obey a binomial distribution. Next, in Sec. III, packings consisting of multiple, binomially distributed, noninteracting, and discretely sized particles are considered. It is furthermore shown that when the size ratio of subsequent particle sizes is constant and tends to unity, these multiple discrete size distributions can be transformed mathematically to a continuously graded system with a lognormal distribution. Subsequently, it is demonstrated that this limit also enables an expression of the void fraction of the lognormal distribution. A general closed-form equation is derived that provides the void fraction as a function of standard deviation, the single-sized void fraction of the particle shape considered (φ_1), and the gradient in void fraction in the limit of a monosized system to a two-component system (β). These properties are physically defined; both φ_1 and β depend on particle shape and mode of packing only. Finally, in Sec. IV, this original expression for the void or packing fraction is compared thoroughly with experiments and computer-generated packing data concerning spherical particles and two sands and found to be in good accordance.

II. PACKING OF PARTICLES WITH A LARGE SIZE RATIO

Furnas [22,27] was the first to model the packing fraction of particle groups with a large size ratio, for which it can be assumed that the particles are not interacting. In this section this type of particle combinations is further elaborated.

A. Saturated packings

Furnas [27] studied binary systems and it was concluded that the greater the difference in size between the two components, the greater the decrease in void volume. It was seen that the binary void fraction h depends on diameter ratio u (d_L/d_S) and on the relative volume fractions of large and small constituents c_L and c_S, whereby for a binary packing obviously holds,

$$c_L = \frac{V_L}{V_L + V_S} = 1 - c_S, \tag{1}$$

where V_L and V_S are the volumes of the large and small constituents in the packing, respectively. The binary packing fraction is defined as

$$\eta(u, c_L) = \frac{V_L + V_S}{V_T} = 1 - h(u, c_L), \tag{2}$$

with h as binary void fraction and V_T as total volume of the packing (entire space), including the voids. Furnas [27] introduced the concept of noninteracting particle classes, i.e., particle groups where the smallest particle of one group is much larger than the largest particle of the other group. Combining the groups implies that they are not interacting. Furnas [27] studied such binary mixtures of particle groups with equal packing fractions.

Now let f_L and φ_L be the packing fraction and void fraction, respectively, of the large particles only and f_S and φ_S of the small component only. The saturated composition, $c_L = c_L^{\text{sat}}$, constitutes a special mix where the concentrations of large and small fractions are such that the small fraction fits exactly in the voids of the large fraction. Hence, by combining two noninteracting size groups, one obtains the total binary packing and void fractions of the saturated packing as follows:

$$\begin{aligned} \eta^{\text{sat}} &= f_L + (1 - f_L) f_S; \\ h^{\text{sat}} &= 1 - \eta^{\text{sat}} = (1 - f_L)(1 - f_S) = \varphi_L \varphi_S, \end{aligned} \tag{3}$$

whereby η^{sat} and h^{sat} stand for $\eta(u > u_b, c_L = c_L^{\text{sat}})$ and $h(u > u_b, c_L = c_L^{\text{sat}})$, respectively. Obviously, this concept is applicable only when the smaller ones do not affect the packing of the larger size group. For such binary packing, the volume fraction of the large fraction in the mix reads as follows:

$$c_L^{\text{sat}} = \frac{f_L}{\eta^{\text{sat}}} = \frac{f_L}{f_L + (1 - f_L) f_S} = \frac{1 - \varphi_L}{1 - \varphi_L + \varphi_L(1 - \varphi_S)}, \tag{4}$$

see Eq. (3) and note that $c_S^{\text{sat}} = 1 - c_L^{\text{sat}}$. Furnas [27] called mixes of binary particles that obey these values of c_L and c_S "saturated mixtures," and in such mixtures the sufficiently small particles are added to just fill the void fraction between the large particles. As noted, the analysis of Furnas [27] was restricted to particle groups that both have the same packing fraction, hence, $\varphi_L = \varphi_S$ (or $f_L = f_S$). In Fig. 1, as an example, both h^{sat} and c_L^{sat} are indicated for $\varphi_L = 0.4$ and $\varphi_S = 0.5$, being 0.2 and 0.75, respectively, see Eqs. (3) and (4).

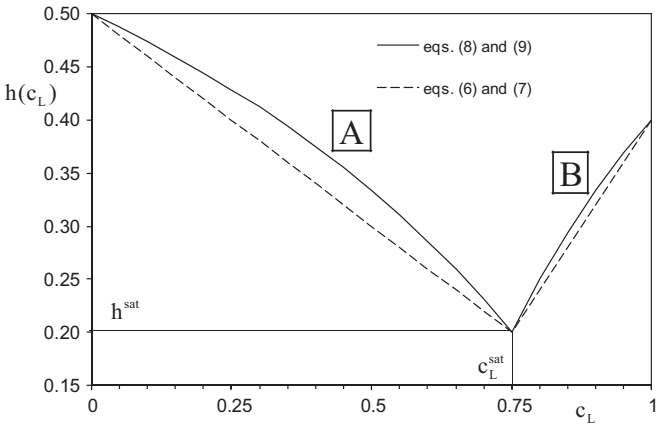

FIG. 1. Binary void fraction, $h(u, c_L)$, of mixes with a large size ratio ($d_L/d_S = u > u_b$) as a function of the volume fraction of large constituent (c_L), with $\varphi_L = 0.4$ and $\varphi_S = 0.5$ as the void fractions of the large and small constituents. The volume fraction (c_L^{sat}) and binary void fraction (h^{sat}) pertaining to a saturated mix are indicated, as well as linear interpolations [Eqs. (6) and (7)] and the curves A or B [Eqs. (8) and (9), respectively] for all other compositions.

Furnas [22] subsequently extended the saturated binary packing model to multiple particle packings, again with each component having the same packing fraction. The major consideration is that the holes of the larger group are filled with the particles of the smaller groups. When the interstices of the smaller particles are filled with smaller ones, the distribution of the particle groups forms a geometrical progression: not only the particles sizes but also the concentration of adjacent size groups has a constant ratio, i.e., a geometric progression is obtained. For particle groups which all have the same individual packing or void fraction, viz. f_1/φ_1, for these saturated or geometric packings the following holds:

$$\varphi_n^{\text{sat}} = \varphi_1^n. \tag{5}$$

For the binary packing of two groups with an identical packing fraction, Eqs. (3) and Eq. (5) with $n = 2$ are compatible indeed (considering that then $\varphi_L = \varphi_S = \varphi_1$).

Experiments with mixtures of broken solids [27] and steel balls [28] revealed that noninteraction between subsequent size groups is obviously true when $u \to \infty$ but that nondisturbance is also closely approximated when $d_L/d_S \approx 7 - 10$ (designated as u_b). For angular particles, Caquot [29] found empirically a comparable size ratio ($u_b \approx 8$–16).

B. Binary packing

In this paper the binary void fractions in the entire concentration range need to be known, not only specifically at the indicated saturation condition. Furnas [27] assumed linear relations between the binary void fraction h and the volume fraction c_L in the ranges $c_L = 0$ and c_L^{sat} and c_L^{sat} and 1, whereby at $c_L = 0$ and $c_L = 1$ the same void fraction prevails, so $\varphi_L = \varphi_S$.

This principle can also be applied to a binary system of which the two components are having different packing

fractions. The linear interpolations read as follows:

$$\eta(u > u_b, c_L) = \frac{(\eta^{\text{sat}} - f_S)c_L}{c_L^{\text{sat}}} + f_S = [f_L + (1 - f_L)f_S](1 - f_S)c_L + f_S; \quad \left(0 \leqslant c_L \leqslant c_L^{\text{sat}}\right), \tag{6}$$

$$\eta(u > u_b, c_L) = \frac{(\eta^{\text{sat}} - f_L)(c_L - 1)}{c_L^{\text{sat}} - 1} + f_L = [f_L + (1 - f_L)f_S](1 - c_L) + f_L; \quad \left(c_L^{\text{sat}} \leqslant c_L \leqslant 1\right), \tag{7}$$

whereby Eqs. (3) and (4) are inserted. Substituting $c_L = c_L^{\text{sat}}$ into Eqs. (6) and (7) indeed yields $\eta = \eta^{\text{sat}}$, and $c_L = 0$ and $c_L = 1$ yield the packing fractions of the small and large components, f_S and f_L, respectively. In Fig. 1 the void fraction following from both lines are added, again using $f_L = 0.6$ ($\varphi_L = 0.4$) and $f_S = 0.5$ ($\varphi_S = 0.5$), the binary void fraction h readily following from Eq. (2).

Expressions for the true packing or void fraction in the entire compositional range were presented by Farr and Groot [30], based on equal packing fractions of both large and small size fractions (so $\varphi_L = \varphi_S$). Kyrylyuk *et al.* [31] derived the packing fractions in case of $\varphi_L \neq \varphi_S$. Here, an alternative derivation of these expressions is presented, yielding the same result.

First, the void fraction for c_L ranging from zero to c_L^{sat} is considered. This is the situation of a particle packing of small particles and their intermediate voids, total volume V_S/f_S, to which a volume V_L of large particles is added which have yet not attained their maximum packing fraction or minimum void fraction, as is the case at the saturation point. The binary packing and void fractions therefore read as follows:

$$\eta(u > u_b, c_L) = \frac{V_L + V_S}{V_L + V_S/f_S} = \frac{f_S}{1 - c_L(1 - f_S)};$$
$$h(u > u_b, c_L) = \frac{(1 - c_L)\varphi_S}{1 - c_L\varphi_S} \quad \left(0 \leqslant c_L \leqslant c_L^{\text{sat}}\right), \tag{8}$$

whereby Eq. (1) is inserted.

The concentration c_L ranging from c_L^{sat} to unity concerns a close packing of large particles, total volume V_L/f_L, to which voids small particles are added, reads as follows:

$$\eta(u > u_b, c_L) = \frac{V_L + V_S}{V_L/f_L} = \frac{f_L}{c_L};$$
$$h(u > u_b, c_L) = \frac{c_L - 1 + \varphi_L}{c_L} \quad \left(c_L^{\text{sat}} \leqslant c_L \leqslant 1\right), \tag{9}$$

where again Eq. (1) has been used. For $c_L = c_L^{\text{sat}}$ Eqs. (8) and (9) yield Eqs. (3). Furthermore, η and h in Eqs. (8) and (9) obey Eq. (2). In Fig. 1, Eqs. (8) and (9) are added, where for convenience they are termed A and B, respectively. Both concave curves are drawn again using $\varphi_L = 0.4$ and $\varphi_S = 0.5$.

Furnas [27] assumed linear relations for the binary packing fraction between the saturated composition and the packing fractions of the two components, invoking identical packing fractions. But in the experimentally constructed binary void graphs also curved lines appear for $u \to \infty$ ([27], see also Ref. [24]), similarly shaped as the concave curves A and B presented in Fig. 1.

Recently, computer-generated packings of binary mixes of unimodal spheres reveal that for $u = 5$, which is still a relatively small size ratio, the numerical values approximate the concave Eq. (9) already within 7% [32,33]. This computational study thus also confirms that u_b is close to 5, being in line with the above-mentioned values from Refs. [27–29]. It is also interesting to note that in Ref. [32] the composition was expressed in the small sphere number fraction x and that their x^{sat} tends to unity for $u \to \infty$, in line with Eq. (4) indeed [33].

C. Binomial distribution of binary and ternary packings

Here the packing of multiple discretely sized particles, with a large size ratio, is studied where their volume fractions obey a binomial distribution. For the binomial distribution of n particle size classes and probability p, their volume fractions for $i = 1, 2, \ldots, n$, are given as

$$c_i = \binom{n-1}{i-1} p^{n-i}(1-p)^{i-1}. \tag{10}$$

Henceforth, in this paper only symmetrical distributions are considered, so $p = ½$. For the binary distribution, $n = 2$, then it follows that $c_1 = c_2 = ½$. For particle groups each having a void fraction $\varphi_1 = \varphi_L = \varphi_S$ (packing fraction $f_1 = f_S = f_L$) the following holds:

$$c_L^{\text{sat}} = \frac{1}{1 + \varphi_1}, \tag{11}$$

see Eq. (4). As $0 \leqslant \varphi_1 \leqslant 1$, Eq. (11) obviously yields $c_L^{\text{sat}} \geqslant ½$, so Eq. (8) (curve A in Fig. 1) applies for this symmetrical binary binomial distribution. By substituting $c_L = ½$ in Eq. (8), for the combined size groups the following holds:

$$f_2^{\text{BN}} = \frac{2f_1}{1 + f_1}; \quad \varphi_2^{\text{BN}} = \frac{\varphi_1}{2 - \varphi_1}, \tag{12}$$

where the symbols f_2^{BN} and φ_2^{BN} replace η and h, respectively, and the superscript BN refers to binomial and the subscript 2 to binary.

For a ternary binomial distribution, $n = 3$, $c_1 = c_3 = ¼$ holds, and $c_2 = ½$, see Eq. (10), whereby $p = ½$. In Fig. 2 the cumulative finer fraction $F(\ln d)$ of such a mix composition, comprising discretely sized particles, is shown graphically. The F of such discrete packing consists of multiple Heaviside functions. At each d_i, F increases with c_i, whereby c_i follows from Eq. (10). In Fig. 2 this is explained graphically for the considered ternary packing. In a frequency distribution graph, at each size group d_i, the population is given by $c_i\ \delta(\ln d_i - \ln d)$, with $\delta(x)$ being the Dirac function. For such a ternary distribution with noninteracting sizes, again Fig. 1 is applicable concerning its void fraction, as explained in what follows.

First, the binary packing of the two smallest components only is considered, d_2 and d_3, which are each smaller than d_1, and each having a packing fraction $\varphi_1 = \varphi_L = \varphi_S$, with composition $c_L = 2/3$ (as $c_3 = ¼$ and $c_2 = ½$). This is permitted as the two smallest components are both noninteracting with the large component (d_1). Depending on the value of φ_1, see Eq. (11), c_L is smaller or larger than c_L^{sat}, and, hence, either curve A or B, respectively, of Fig. 1 applies. From Eq. (11)

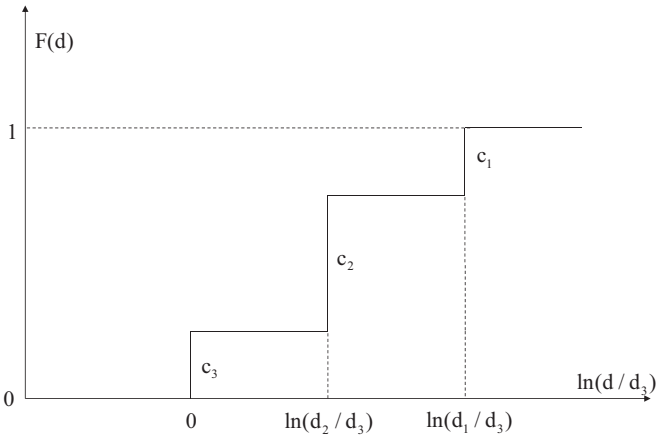

FIG. 2. Cumulative finer fraction F versus the logarithm of the scaled particle size for a discretely sized ternary mix (with $d_1/d_2 = d_2/d_3 = u$) having a binomial distribution ($p = ½$) of the particle volumes and, hence, $c_1 = 0.25$, $c_2 = 0.5$, and $c_3 = 0.25$.

it follows that for $\varphi_1 \leq ½$, $c_L = 2/3 \leq c_L^{\text{sat}}$ and curve A is applicable, whereas for $\varphi_1 \geq ½$, $c_L \geq c_L^{\text{sat}}$ and curve B is applicable.

Hence, substituting $c_L = 2/3$ in Eqs. (8) and (9) produces

$$f_{23} = \frac{3f_1}{1+2f_1}; \quad \varphi_{23} = \frac{\varphi_1}{3-2\varphi_1} \quad (0 \leqslant \varphi_1 \leqslant ½);$$
$$f_{23} = \frac{3f_1}{2}; \quad \varphi_{23} = \frac{3\varphi_1 - 1}{2} \quad (½ \leqslant \varphi_1 \leqslant 1). \tag{13}$$

Next this binary arrangement is combined with the largest component with size d_1. This combination can be considered as a bimodal mix of the two small components (namely combined d_2 and d_3) with Eq. (13) as packing (void) fraction f_S (φ_S) on the one hand, and the large component d_1 with packing (void) fraction $f_L = f_1$ ($\varphi_L = \varphi_1$) on the other, with composition $c_L = ¼$.

Equation (4) and using the two possible f_{23} [Eq. (13)] as f_S, and f_1 as f_L, reveals that for all φ_1 holds $c_L = ¼ \leqslant c_L^{\text{sat}}$, so curve A [Eq. (8)] applies as follows:

$$f_3^{\text{BN}} = \frac{4f_{23}}{3+f_{23}} = \frac{4f_1}{1+3f_1};$$
$$\varphi_3^{\text{BN}} = \frac{\varphi_1}{4-3\varphi_1} \quad (0 \leqslant \varphi_1 \leqslant ½), \tag{14}$$
$$f_3^{\text{BN}} = \frac{4f_{23}}{3+f_{23}} = \frac{4f_1}{2+f_1};$$
$$\varphi_3^{\text{BN}} = \frac{3\varphi_1 - 1}{3-\varphi_1} \quad (½ \leqslant \varphi_1 \leqslant 1), \tag{15}$$

The obtained binary [Eq. (11)] and ternary [Eqs. (14) and (15)] void fractions, referred to as φ_n^{BN}, of the binomial arrangements of noninteraction groups are included in Table I, which are a function of the void fraction φ_1 of the individual size group only.

III. BINOMIAL AND LOGNORMAL DISTRIBUTIONS

In this section, first the packing of binomially distributed noninteracting particle groups is addressed. Next, the binomial particle packing of single sized particles, invoking a constant size ratio, is transformed into a continuous lognormal-distributed packing. It will be seen that the binary discrete packing, in the limit of the size ratio u tending to unity, plays a key role in the derivation of the packing fraction of this distribution.

A. Binomial distributions of single-sized particles with a large size ratio

Using the same reasoning as for the binary and ternary arrangements in the previous section, also the binomial void fractions of multiple size groups, φ_n^{BN}, for which the subsequent sizes do not interact, can be determined. The expressions up to 10 size groups ($n = 10$) are included (Table I), and the underlying computation for $n = 8$ is included

TABLE I. Void fraction φ_n^{BN} of particle mixes consisting of n particle classes with a large size difference between the subsequent classes ($u > u_b$), whereby the classes are binomially distributed, and each particle class has a void fraction φ_1.

n	φ_n^{BN}
1	φ_1 $(0 \leqslant \varphi_1 \leqslant 1)$
2	$\frac{\frac{1}{2}\varphi_1}{1-\frac{1}{2}\varphi_1}$ $(0 \leqslant \varphi_1 \leqslant 1)$
3	$\frac{\varphi_1}{4-3\varphi_1}$ $(0 \leqslant \varphi_1 \leqslant 1/2)$; $\frac{3\varphi_1-1}{3-\varphi_1}$ $(1/2 \leqslant \varphi_1 \leqslant 1)$
4	$\frac{\varphi_1}{8-7\varphi_1}$ $(0 \leqslant \varphi_1 \leqslant 1/3)$; $\frac{4\varphi_1-1}{7-4\varphi_1}$ $(1/3 \leqslant \varphi_1 \leqslant 1)$
5	$\frac{\varphi_1}{16-15\varphi_1}$ $(0 \leqslant \varphi_1 \leqslant 1/4)$; $\frac{5\varphi_1-1}{15-11\varphi_1}$ $(1/4 \leqslant \varphi_1 \leqslant 2/3)$; $\frac{11\varphi_1-5}{11-5\varphi_1}$ $(2/3 \leqslant \varphi_1 \leqslant 1)$
6	$\frac{\varphi_1}{32-31\varphi_1}$ $(0 \leqslant \varphi_1 \leqslant 1/5)$; $\frac{6\varphi_1-1}{31-26\varphi_1}$ $(1/5 \leqslant \varphi_1 \leqslant 1/2)$; $\frac{8\varphi_1-3}{13-8\varphi_1}$ $(1/2 \leqslant \varphi_1 \leqslant 1)$
7	$\frac{\varphi_1}{64-63\varphi_1}$ $(0 \leqslant \varphi_1 \leqslant 1/6)$; $\frac{7\varphi_1-1}{63-57\varphi_1}$ $(1/6 \leqslant \varphi_1 \leqslant 2/5)$; $\frac{22\varphi_1-7}{57-42\varphi_1}$ $(2/5 \leqslant \varphi_1 \leqslant 3/4)$; $\frac{21\varphi_1-11}{21-11\varphi_1}$ $(3/4 \leqslant \varphi_1 \leqslant 1)$
8	$\frac{\varphi_1}{128-127\varphi_1}$ $(0 \leqslant \varphi_1 \leqslant 1/7)$; $\frac{8\varphi_1-1}{127-120\varphi_1}$ $(1/7 \leqslant \varphi_1 \leqslant 1/3)$; $\frac{29\varphi_1-8}{120-99\varphi_1}$ $(1/3 \leqslant \varphi_1 \leqslant 3/5)$; $\frac{64\varphi_1-29}{99-64\varphi_1}$ $(3/5 \leqslant \varphi_1 \leqslant 1)$
9	$\frac{\varphi_1}{256-255\varphi_1}$ $(0 \leqslant \varphi_1 \leqslant 1/8)$; $\frac{9\varphi_1-1}{255-247\varphi_1}$ $(1/8 \leqslant \varphi_1 \leqslant 3/7)$; $\frac{93\varphi_1-37}{219-163\varphi_1}$ $(3/7 \leqslant \varphi_1 \leqslant 4/5)$; $\frac{163\varphi_1-93}{163-93\varphi_1}$ $(4/5 \leqslant \varphi_1 \leqslant 1)$
10	$\frac{\varphi_1}{512-511\varphi_1}$ $(0 \leqslant \varphi_1 \leqslant 1/9)$; $\frac{10\varphi_1-1}{511-502\varphi_1}$ $(1/9 \leqslant \varphi_1 \leqslant 1/4)$; $\frac{23\varphi_1-5}{251-233\varphi_1}$ $(1/4 \leqslant \varphi_1 \leqslant 3/7)$; $\frac{65\varphi_1-23}{233-191\varphi_1}$ $(3/7 \leqslant \varphi_1 \leqslant 2/3)$; $\frac{128\varphi_1-65}{191-128\varphi_1}$ $(2/3 \leqslant \varphi_1 \leqslant 1)$

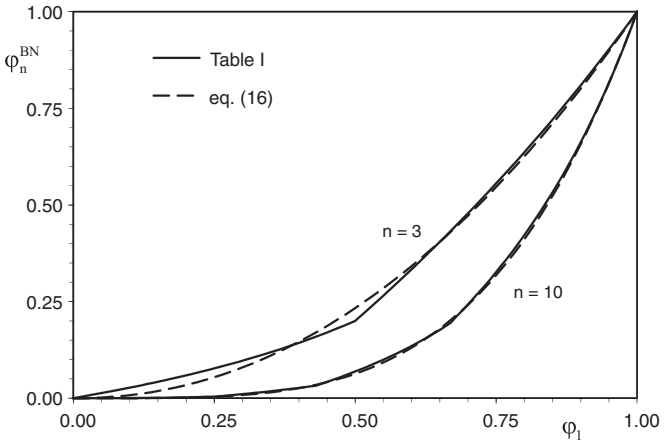

FIG. 3. Void fraction φ_n^{BN} of binomially distributed combinations of noninteracting particle classes as a function of the void fraction φ_1 of each particle class for $n = 3$ and $n = 10$, taken from Table I, and following Eq. (16) with ψ_n, taken from Table II (fitted value).

in the Appendix. In Fig. 3, as an example, the binomial void fractions for $n = 3$ and 10 are set out versus φ_1.

Note that for the derivation of these expressions each particle class does not need to be monosized (so it may be polydisperse), and their size ratio does need to be constant; the only requirement is that each class has the same packing (or void) fraction and that the size ratio between subsequent groups is sufficiently large so they are all noninteracting.

Analogously to the void fraction of saturated (geometrically) composed mixes, it appears that the void fraction of the binomial arrangements also approximates a power function,

$$\varphi_n^{BN} = \varphi_1^{\psi_n}. \tag{16}$$

For the number of size groups n ranging from 2 to 10 this power equation is fitted to the expressions of Table I, and the coefficients ψ_n are included in Table II. The pertaining regression coefficient is 0.996 for $n = 2$ and increases with augmenting n and is 0.999 for $n = 10$. These values and their trend confirm that the binomial expressions (Table I) can be described by a power model, which becomes more accurate at higher n (see also Fig. 3). In the following, in the limit of large n, an analytical expression for ψ_n is derived.

TABLE II. Values of ψ_n following a fit of Eq. (17) to the void fractions of Table I, and gradients of these void fractions at $\varphi_1 = 0$ and $\varphi_1 = 1$, for varied n.

n	ψ_n (fit)	$\left.\frac{d\varphi_n^{BN}}{d\varphi_1}\right\|_{\varphi_1=0}$	$\left.\frac{d\varphi_n^{BN}}{d\varphi_1}\right\|_{\varphi_1=1}$	$\sqrt{\frac{\pi(n-1)}{2}}$	$\sqrt{\frac{\pi n}{2}}$
1	1.00	2^{-0}	1	0.000	1.253
2	1.60	2^{-1}	2	1.253	1.772
3	2.10	2^{-2}	2	1.772	2.171
4	2.38	2^{-3}	8/3	2.171	2.507
5	2.75	2^{-4}	8/3	2.507	2.802
6	2.98	2^{-5}	16/5	2.802	3.070
7	3.28	2^{-6}	16/5	3.070	3.316
8	3.48	2^{-7}	128/35	3.316	3.545
9	3.75	2^{-8}	128/35	3.545	3.760
10	3.98	2^{-9}	256/63	3.760	3.963

First, the gradients of the binomial void fractions at $\varphi_1 = 0$ and $\varphi_1 = 1$ are listed in Table II. These gradients of approximate Eq. (16) at $\varphi_1 = 0$ and $\varphi_1 = 1$ read

$$\left.\frac{d\varphi_n^{BN}}{d\varphi_1}\right|_{\varphi_1=0} = 0; \quad \left.\frac{d\varphi_n^{BN}}{d\varphi_1}\right|_{\varphi_1=1} = \psi_n. \tag{17}$$

The true gradient at $\varphi_1 = 0$ is 2^{1-n} (Table II) and is therefore exponentially tending to zero with increasing n, as is the case with Eqs. (16) and (17).

For odd n, Table I reveals that near $\varphi_1 = 1$

$$\varphi_n^{BN} = \frac{a\varphi_1 - b}{a - b\varphi_1}, \tag{18}$$

and, hence,

$$\left.\frac{d\varphi_n^{BN}}{d\varphi_1}\right|_{\varphi_1=1} = \frac{a+b}{a-b} = \frac{2^{n-1}}{\binom{n-1}{\frac{n-1}{2}}} \to \sqrt{\frac{\pi(n-1)}{2}} \quad (n \to \infty), \tag{19}$$

as

$$a = \sum_{i=0}^{\frac{n-1}{2}} \binom{n-1}{i} = 2^{n-2} + \frac{1}{2}\binom{n-1}{\frac{n-1}{2}}; \quad b = 2^{n-1} - a, \tag{20}$$

and the Catalan number C_n holds as follows [34]:

$$C_n = \frac{1}{n+1}\binom{2n}{n} \to \frac{2^{2n}}{(n+1)\sqrt{n\pi}} \quad (n \to \infty). \tag{21}$$

For $n = 4$, 8, etc., Table I reveals that near $\varphi_1 = 1$

$$\varphi_n^{BN} = \frac{a\varphi_1 - b}{2a - b - a\varphi_1}, \tag{22}$$

and, hence,

$$\left.\frac{d\varphi_n^{BN}}{d\varphi_1}\right|_{\varphi_1=1} = \frac{2a}{a-b} = \frac{2^{n-1}}{\binom{n-1}{\frac{n}{2}}} = \frac{2^n}{\binom{n}{\frac{n}{2}}} \to \sqrt{\frac{\pi n}{2}} \quad (n \to \infty), \tag{23}$$

as

$$a = 2^{n-2};$$
$$2a - b = \frac{1}{2}\sum_{i=0}^{n-1}\binom{n-1}{i} + \binom{n-1}{\frac{n}{2}} = 2^{n-2} + \binom{n-1}{\frac{n}{2}}, \tag{24}$$

and applying Eq. (21). Also for $n = 2$, 6, 10, etc. Eq. (22) holds, but here Table I reveals that

$$a = 2^{n-3};$$
$$2a - b = \frac{1}{4}\sum_{i=0}^{n-1}\binom{n-1}{i} + \frac{1}{2}\binom{n-1}{\frac{n}{2}} = 2^{n-3} + \frac{1}{2}\binom{n-1}{\frac{n}{2}}, \tag{25}$$

and, hence, applying Eq. (21), again Eq. (23) is obtained.

So for large n, it appears that ψ_n asymptotically tends to $\sqrt{\pi(n-1)/2}$ and $\sqrt{\pi n/2}$ for odd and even n, respectively, with the difference vanishing with increasing values of n. For finite values of n, Table I shows that $\sqrt{\pi n/2}$ matches the exact value of ψ_n quite accurately for $n = 2$; the difference is about 10%, and for $n = 3$ it is already reduced to 3%, and it reduces further with increasing n. To conclude, where multicomponent geometrical packings have a void fraction of φ_1^n for all n [23], binomial distributions tend to a void fraction of $\varphi_1^{\sqrt{\pi n/2}}$ for large n, whereby this expression also approximately holds for values of n as low as 2. In the next section the void fraction is derived in the case the number of particle sizes is increased, and size ratio (u) between subsequent particle sizes is equal and tending to unity, i.e., a continuous lognormal size distribution is obtained.

B. Transformation into lognormal distribution

The void fraction of saturated packings consisting of multiple noninteracting particle classes with a binomial distribution was given by Eq. (16). Here, the void fraction of the polydisperse continuous (lognormal law) packing is addressed.

For the binomial distribution, when all size ratios u are constant and the particle groups are monosized, the standard deviation $\ln\sigma_g$ and geometric mean size d_g read as follows:

$$\ln\sigma_g = \sqrt{(n-1)p(1-p)}\ln u, \tag{26}$$

$$\ln(d_g/d_n) = (n-1)p\ln u, \tag{27}$$

with σ_g as geometric standard deviation.

Adding more monosized particle classes, each subsequent class having the same size ratio, and letting $u \to 1$ and following the DeMoivre-Laplace limit theorem (e.g., see Ref. [35]), the binomial distribution turns into a continuous lognormal distribution. Here the logarithm of the particle size class is namely binomially or normally distributed (as size ratios are relevant), which means that a lognormal distribution of the particle size is obtained for $u \to 1$, for a lognormal distribution is a continuous probability distribution of a random variable whose logarithm is normally distributed. Hence, the cumulative finer fraction (or distribution function) of the particles volume reads as follows:

$$F(d) = \frac{1}{\sqrt{2\pi}\ln\sigma_g}\int_{-\infty}^{d}\exp\left[-\frac{(\ln d - \ln d_g)^2}{2\ln^2\sigma_g}\right]d(\ln d). \tag{28}$$

With d_g (or d_{50}) as geometric mean size of the distribution, σ_g as the geometric standard deviation, and $\ln\sigma_g$ as the standard deviation.

For small size ratio, so for $u \to 1$, using $c_L = p$ [Eq. (10)], the binary void fraction $h(u, p)$ [23,24,34] reads as follows:

$$h(u, p) = \varphi_1 - 4\beta\varphi_1(1-\varphi_1)(1-p)p\ln u, \tag{29}$$

So far, the packing perturbation generated by a size ratio unequal to unity has been expressed both in $u - 1$ and $(u^3 - 1)/3$ [23,24,34], while here $\ln u$ is chosen, and all three expressions provide the same first-order perturbation and, hence, gradient at $u = 1$, relevant for continuous packings, and are therefore equivalent for $u \to 1$.

TABLE III. Experimental values for monosized void and packing fraction and β for various particle shapes and their mode of packing [23]. The sphericity is the Wadell sphericity [25].

Material	Packing	Shape	f_1	φ_1	β
Steel	RCP	Spherical	0.64	0.36	0.20
Sand (OR)	RCP	Sphericity = 0.86	0.624	0.376	0.25
Sand (MR)	RCP	Sphericity = 0.81	0.574	0.426	0.26
Quartz	RCP	Fairly angular	0.503	0.497	0.373
Feldspar	RCP	Plate-shaped	0.497	0.503	0.374
Dolomite	RCP	Fairly rounded	0.495	0.505	0.347
Sillimanite	RCP	Distinctly angular	0.469	0.531	0.395

Equation (29) readily reveals that near $u = 1$ the packing extremum is obtained when the two class concentrations are in parity, $p = 0.5$. Likewise φ_1, for disordered packings, β depends only on the packing mode of the mix (loose, dense, etc.) and the particle shape, so it is a given and nonadjustable parameter. This also holds for ordered packings of spheres in which the spheres are randomly placed, in which case $\beta\varphi_1 = -¾$ [36]. In Table III, known values of φ_1 and β for disordered packings are summarized.

As stated, in the limit of infinitesimal increments the packing of discretely sized particles transforms to the lognormal size distribution. This infinite-particle-sizes approach can be employed to derive the void fraction of the lognormal distribution, following a similar approach as in Ref. [23] for geometric packings.

Equation (16) and Table II show that the void fraction is reduced proportionally to the square root of the number of size groups and is in one part of the packing the same as in any other part. When the size ratio u between the adjacent sizes is smaller than u_b, the concept concerning smaller particles packing perfectly in the voids of the larger ones does not hold anymore, but also, in this case, the void fraction reduction involved with the size ratio of adjacent size groups (of constant ratio) is the same in any part of the packing. Accordingly, for a system with n size groups and small u is proposed:

$$\varphi_n^{\mathrm{BN}}(u, p) = \varphi_1\left(\frac{h(u,p)}{\varphi_1}\right)^{\psi_n - \psi_2 + 1} \approx \varphi_1\left(\frac{h(u,p)}{\varphi_1}\right)^{\sqrt{\pi n/2} - \sqrt{\pi} + 1}. \tag{30}$$

Following this principle, adding more size groups to the mix with a certain size range will reduce the void fraction. But, on the other hand, its effect is less as the size ratio of adjacent groups tends to unity (i.e., $u \to 1$) and the resulting void fraction of adjacent size groups, governed by $h(u, p)$, tends to φ_1.

For geometric packings the power in the void fraction reduction, ψ_n, appeared to be equal to n, so applying this multiple interacting particle principle led to a power of $n - 1$. This equation was successfully validated for a finite number of spheres ($n = 3$) with finite size ratio ($u = 2$) [24] and for an infinite number of particles with $u \downarrow 1$, i.e., a continuous distribution [23].

Now the effect of adding an infinite number of size groups, resulting in a continuous lognormal packing on the void

fraction can be quantified as well. Adding more size groups to the mix will reduce the void fraction asymptotically with a power $\sqrt{n}$, see Eqs. (16) and (30), with $\psi_n = \sqrt{\pi n/2}$ for large n. However, its effect is lessened as the correction of φ_1 tends to unity as $h(u, p)$, tends to φ_1, see Eq. (29). For a system with n size groups, using Eq. (26) and $p = ½$, Eqs. (29) and (30) yield the following:

$$\varphi^{\mathrm{LN}} = \varphi_1 \lim_{n\to\infty}\left[1 - \frac{2\beta(1-\varphi_1)\ln\sigma_g}{\sqrt{n-1}}\right]^{\sqrt{\pi n/2}-\sqrt{\pi}+1}$$

$$= \varphi_1 \exp[-\sqrt{2\pi}\beta(1-\varphi_1)\ln\sigma_g] = \varphi_1 \sigma_g^{-\sqrt{2\pi}\beta(1-\varphi_1)}. \quad (31)$$

For the outcome of the limit it is not relevant whether for ψ_2 in Eqs. (30) and (31) is taken the value 1.60, 1.772 or 2 (Table II). Equation (31) provides the void fraction of a continuous lognormal distribution, which depends on the void fraction of the single-sized particles (φ_1), the standard deviation ($\ln\sigma_g$), and the maximum gradient of the single-sized void fraction on the onset to binary packing (β), which are all specified properties. The packing fraction readily follows as

$$f^{\mathrm{LN}} = 1 - \varphi_1 \exp[-\sqrt{2\pi}\beta(1-\varphi_1)\ln\sigma_g]$$

$$= 1 - \varphi_1 \sigma_g^{-\sqrt{2\pi}\beta(1-\varphi_1)}. \quad (32)$$

The geometric mean size does not feature in Eqs. (31) and (32) because its variation only implies a multiplication of the size of all particles with the same factor. As void fractions are determined by relative particle sizes, this does not affect the void fraction. Equation (31) furthermore indicates that the void fraction of the system tends to the monosized void fraction when the standard deviation tends to zero, i.e., the distribution tending to a monosized distribution, as would be expected. For small $\ln\sigma_g \to 0$, Eq. (31) can be expanded as up to the quadratic term as follows:

$$\varphi^{\mathrm{LN}} = \varphi_1[1 - \sqrt{2\pi}\beta(1-\varphi_1)\ln\sigma_g + \pi[\beta(1-\varphi_1)\ln\sigma_g]^2 + O(\ln^3\sigma_g)]. \quad (33)$$

By using $f^{\mathrm{LN}} = 1 - \varphi^{\mathrm{LN}}$, the approximate solution for the packing fraction is also obtained. Equation (33) reveals that the second-order term has a sign opposite that of the first-order term. This reflects that the initial linear void fraction reduction (packing increase) flattens with increasing $\ln\sigma_g$ (more polydispersity), which is in line with the asymptote that is approached for infinite $\ln\sigma_g$, namely a void fraction of zero (a packing fraction of unity).

IV. COMPARISON WITH REPORTED DATA

A thorough verification of Eq. (30), concerning a finite number ($n = 3$) of binomially distributed interacting particles with finite size ratio ($u = 2$) is presented here. Furthermore, a verification of Eqs. (31) and (32) is possible by comparing them with computational and experimental packing data of lognormal distributions reported in the literature [11,12,25,26,37]. This data concern packings of spheres and nonspherical particles, packed from random loose to random close. The monosized packing values readily follows from their packing fraction at $\ln\sigma_g = 0$. Likewise φ_1, for disordered packings, β depends only on the packing mode of the mix (loose, dense, etc.) and the particle shape, so it is a given and nonadjustable parameter as well. It is assumed that the retrieved data concerning all simulated and measured polydisperse systems reported in the literature have the same degree of compaction as in the pertaining monosized case, which is also assumed implicitly by Refs. [11,12,25,26,37], so φ_1 and β are applicable for all $\ln\sigma_g$.

A. Discretely sized sphere packings with finite size ratio

The empirical ternary (monosized) sphere packing results of Jeschar *et al.* [38] are considered, but they did not specify how their packings were prepared and measured. They obtained $\varphi_1 = 0.366$ for the monosized packing of spheres with diameters 7 mm (d_3), 14 mm (d_2), and 28 mm (d_1). These values are compatible with RCP values from other experiments [8] and with computer-generated values [9–14]. Equation (30) is, however, applicable to any mode of packing, from random loose to random close packed. To apply the current multiple particles packing model, unimodal, binary, and ternary packings only need to be prepared and compacted in a comparable way.

The binary and ternary packing results from Ref. [38] are summarized in a ternary plot, which can also be found elsewhere [24]. The sides of the triangle show that the binary packings of 7 and 14 mm have the same void fraction as the mixes of 14 and 28 mm packing at equal compositions, which would be expected as the size ratios of these binary mixtures are equal ($d_1/d_2 = d_2/d_3 = u = 2$). These measured binary void fractions h are included in Table IV for various compositions (c_L or p).

The compatible unimodal void fractions as measured with the three individual spheres sizes, as well as the compatible binary void fractions measured with d_1/d_2 and d_2/d_3 mixes,

TABLE IV. Binary void fraction of monosized spheres, $h(u, p)$, as measured by Ref. [38] concerning $u = 2$, for which the probability corresponds to the volume fraction of large constituent (corresponding to c_L), the measured ternary void fraction $j(u, p)$ [38], and the ternary void fraction $j(u, p)$ computed using Eq. (30). The monosized void fraction $\varphi_1 = 0.366$.

p	h [38]	j [38]	j [Eq. (30)]
0	0.366	0.366	0.366
0.1	0.358		0.356
0.2	0.351		0.346
0.25		0.335	
0.3	0.346		0.339
0.4	0.340		0.331
0.5	0.335	0.332	0.324
0.6	0.335		0.324
0.7	0.335	0.321	0.324
0.75		0.322	
0.8	0.341		0.332
0.85		0.325	
0.9	0.352		0.347
1	0.366	0.366	0.366

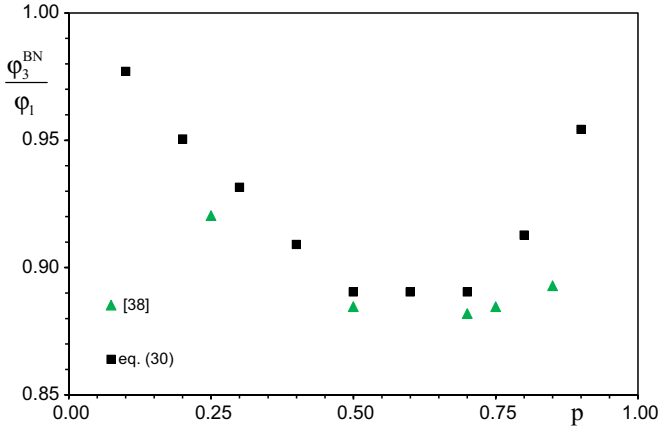

FIG. 4. (Color online) Scaled ternary void fraction of spheres ($u = 2$) versus the probability as measured [38] and as computed by Eq. (30) with substituting $n = 3$ and using the scaled binary void fraction ($u = 2$) as measured [38]. The values are summarized in Table IV.

indicate that Jeschar *et al.* [38] conducted all their experiments in a reproducible and robust manner.

Using the void fraction of binomial ternary packings ($n = 3$) that can be extracted from [38], it can now be verified if Eq. (30) is applicable. In Table IV the compositions of ternary binomial packings with five different p are included, for which c_i follows from Eq. (10). The pertaining ternary void fraction $j(u, p)$ of each packing as measured by Ref. [38] is taken from the ternary diagram and is included in Table IV as well. Finally, the ternary void fraction is computed using Eq. (30), substituting $n = 3$ yields a power of 1.40 ($=\sqrt{3\pi/2} - \sqrt{\pi} + 1$), and the corresponding binary void fraction $h(u, p)$ is also taken from Table IV. Comparing the values predicted by Eq. (30) and the measured values, see Table IV, reveals that the ternary packing fraction can be predicted accurately from the binary void fraction $h(u, p)$ using Eq. (30). In Fig. 4 the scaled ternary void fraction as measured in Ref. [38] and computed using Eq. (30), and taking the values from Table IV, are shown graphically. Also, this figure clearly shows the applicability of Eq. (30) in predicting the void fraction of multiple sphere packings (here $n = 3$) using the void fraction of the binary packing. It is also noteworthy to mention that the agreement is even better when the expression with the original power, $\psi_3 - \psi_2 + 1$, in Eq. (30) is used. This power amounts to 1.5; see Table II for the applicable ψ_2 and ψ_3 values.

B. Continuous sphere packings

For mixtures of spheres with lognormal distribution, the packing fractions of arrangements from random loose to random close packing are reported. Spheres (and nonspherical particles) possess a monosized packing fraction that depends on the method of packing (from RLP to RCP). For RCP of uniform spheres the packing fraction (f_1) was experimentally found to be 0.64 [8], in line with computer-generated values [9–13]. The β^{rcp} of RCP is about 0.20 and in Ref. [36] as β of a nonclose random packing was proposed,

$$\beta^{rp}\left(1-f_1^{rp}\right) = \beta^{rcp}\left(1-f_1^{rcp}\right). \tag{34}$$

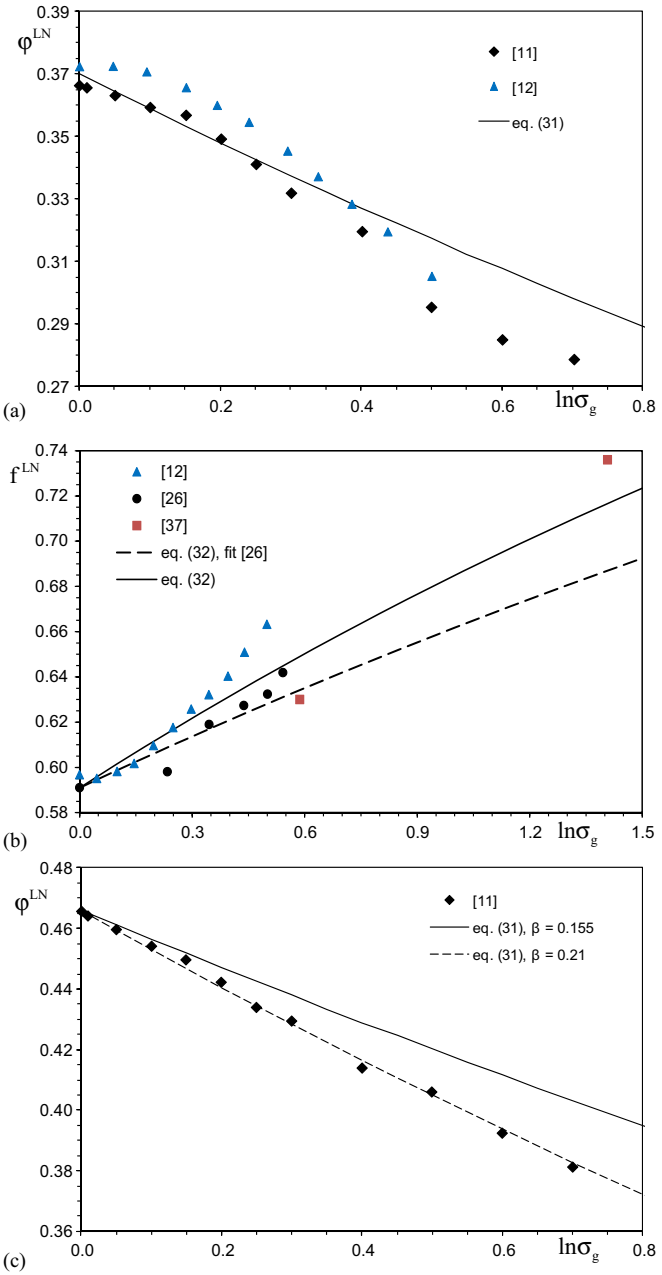

FIG. 5. (Color online) (a) Computer-generated void fraction of random close packed spheres φ^{LN}, with a lognormal size distribution, versus the standard deviation [11,12]. Equation (31) with $\varphi_1 = 0.37$ and where $\beta = 0.195$ is also set out. (b) Experimentally measured [26,37] and computer-generated [12] packing fraction of spheres, with a lognormal size distribution, versus the standard deviation. Equation (32) with $\varphi_1 = 0.409$ and where $\beta = 0.176$ is also set out, as well as with $\sqrt{2\pi}\beta(1-\varphi_1) = 0.19$, which was conjectured in Ref. [26]. (c) Computer-generated void fraction of random loose packed spheres φ^{LN} [11], with a lognormal size distribution, versus the standard deviation. Equation (31) with $\varphi_1 = 0.466$ and where $\beta = 0.155$ and $\beta = 0.21$ are also set out.

Simulations of lognormal size distributed spheres which were close to RCP were reported by Refs. [11,12], and the resulting void fraction can be found in Fig. 5(a), where $f_1 = 0.63$ ($\varphi_1 = 0.37$) and, hence, Eq. (34) yields $\beta = 0.195$.

The monosized packing values readily follow from their packing fraction at $\ln\sigma_g = 0$. In this figure also Eq. (31) is drawn, using $\varphi_1 = 0.37$ and $\beta = 0.195$. One can see that in a large range of standard deviation $\ln\sigma_g$, Eq. (31) is in fair agreement with the computer-generated values of the void fraction. The simulations of Ref. [12] indicate a lower void fraction for small $\ln\sigma_g$, which might be explained by the employed computational method. The simulations in Ref. [11], for instance, approached the commonly accepted monosized RCP void value of about 0.36 (0.363 [11] versus 0.375 [12]). Furthermore, the computational method used in Ref. [11] correctly predicts an almost constant coordination number (of value 6) with increasing $\ln\sigma_g$, and in Ref. [12] it drops significantly. The finding in Ref. [11] is compatible with those in Refs. [39,40] concerning coordination numbers in continuous distributions (among others the lognormal distribution).

Packings with a lower packing fraction, $f_1 = 0.59$ ($\varphi_1 = 0.41$) and $\beta = 0.176$ [Eq. (34)], were considered by both Ref. [26] and Ref. [12], the former experimentally and the latter computationally. In Fig. 5(b) the reported packing fractions f^{LN} are included. The actual standard deviations, corresponding to the packing fractions measured by Dexter and Tanner [26], were computed using their given mix compositions. It appeared that this computed $\ln\sigma_g$ were slightly smaller than the values given by the authors [26], who confirmed that their targeted largest standard deviations could not be fully realized due to the limited range of available ball sizes. As the difference augments with increasing $\ln\sigma_g$, it can most probably be attributed to the truncation of the composed distributions indeed. Table V lists the standard deviations given in Ref. [26], the measured packing fraction, as well as the actual standard deviation computed here based on their "Table 1".

Substituting $f_1 = 0.59$ ($\varphi_1 = 0.41$) and $\beta = 0.176$ in Eq. (32) yields $-0.26\ \ln\sigma_g$ as the exponent featuring in this equation. The authors [26] also suggested an empirical correlation, which is similar to Eq. (32), but with $-0.19\ \ln\sigma_g$ as the exponent of the Euler number. Both equations are shown in Fig. 5(b), and while they both approach unity for infinitely large $\ln\sigma_g$, Eq. (31) with $-0.26\ \ln\sigma_g$ matches the empirical data better. In this graph the simulations by Ref. [12] are also included, and it is obvious that they predict an even larger packing fraction increase with augmenting $\ln\sigma_g$, which was also seen in Fig. 5(a).

The packing of spheres with a wider lognormal distribution were measured by Hunger [37] using a standardized Rigden device for compaction. Glass beads with $d_{10} = 14.8\ \mu$m and $d_{90} = 66.6\ \mu$m, whereby d_x is defined as $\exp(F^{-1}(x\%))$, with F^{-1} as the inverse distribution function or quantile function. For the powder coal fly ash (type a) it was verified that its particles were spherical indeed [37], and for this material $d_{10} = 1.6\ \mu$m and $d_{90} = 59\ \mu$m. The measured packing fractions of compacted glass beads and fly ash amounted to 0.63 and 0.74, respectively.

TABLE V. Standard deviations and packing fractions of the composed lognormal sphere packings as given by Ref. [26] and their recomputed standard deviations based on the size distribution provided by these authors.

$\ln\sigma_g$ [26]	f^{LN} [26]	$\ln\sigma_g$
0	0.591	0
0.230	0.598	0.234
0.345	0.619	0.345
0.461	0.627	0.438
0.576	0.632	0.501
0.691	0.642	0.541

The quantile function of Eq. (28) reads

$$F^{-1}(x\%) = \ln d_g + \sqrt{2}\ln\sigma_g\ \mathrm{erf}^{-1}(2x\% - 1), \tag{35}$$

with erf^{-1} as inverse error function. Using Eq. (35) it follows from $F^{-1}(90\%) - F^{-1}(10\%)$ that

$$\ln\sigma_g = \frac{\ln(d_{90}/d_{10})}{2\sqrt{2}\mathrm{erf}^{-1}(0.8)} = \frac{\ln(d_{90}/d_{10})}{2.563}, \tag{36}$$

as $\mathrm{erf}^{-1}(-x) = -\ \mathrm{erf}^{-1}(x)$ and $\mathrm{erf}^{-1}(0.8) = 0.906$. The resulting standard deviations of glass beads and fly ash are 0.59 and 1.41, respectively. The standard deviations and the respective packing values of both materials are included in Fig. 5(b).

The standard deviation of glass beads is nonzero, while their packing fraction (0.63) is smaller than the random close packing fraction of monosized spheres ($\approx$0.64). From this one can conclude that with the Rigden device a close packing is obtained but that random close packing is not achieved. The agreement of the glass beads value with the steel balls packing values of Dexter and Tanner [26], see Fig. 5(b), at equal standard deviations indicates that similar compaction rates are obtained. Figure 5(b) furthermore reveals that Eq. (32) is in line with the values of both materials, and the fly ash data are particularly interesting as this material features a relatively large standard deviation.

Random loose packings of lognormal distributions were simulated by Ref. [11], for which they generated $f_1 = 0.53$ ($\varphi_1 = 0.47$) and, hence, $\beta = 0.155$ [Eq. (34)]. In Fig. 5(c) their void fractions and the values computed using Eq. (31) are depicted. Again it can be seen that simulations of φ^{LN} and Eq. (31) agree fairly well and that the simulations in Ref. [11] predict a larger void fraction reduction (packing increase) than Eq. (31), which was also seen in Fig. 5(a). Actually, Fig. 5(c) shows that the simulation of Ref. [11] matches very well with Eq. (31) when $\beta = 0.21$ is substituted, a β value which is larger than that of RCP. As β is expected to be smaller when the packing is less close [23,36], the simulations of Ref. [11] feature a larger void fraction reduction than expected. This might indicate that the spheres are closely packed but that the lower void fraction is caused by larger voids created by bridging. This conjecture is supported by their mean coordination number of 6, which is close to that of RCP. In other words, their loose packing simulations have more similarities to their RCP pendants than expected.

Considering Figs. 5(a)–5(c), one can see that Eqs. (31) and (32) provide a good prediction of the sphere void or packing fraction versus a wide range of standard deviations and for various packing modes. To apply these analytically exact expressions, no fitting parameters were needed.

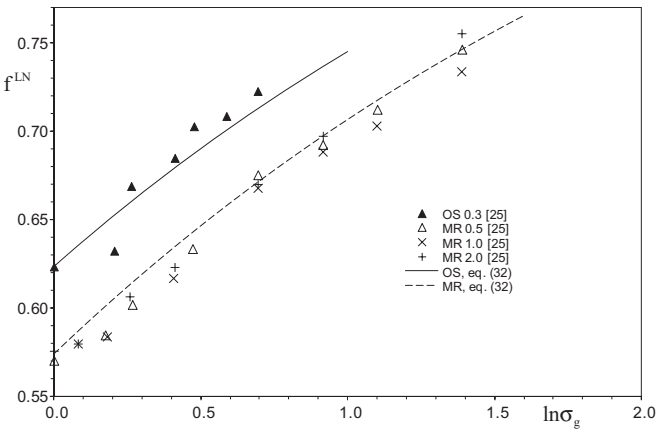

FIG. 6. Experimentally measured packing fraction of two sands (OS and MR), with a lognormal size distribution for different geometric mean sizes d_g (in mm), versus the standard deviation [25]. Equation (32) with $f_1 = 0.576$ and $\beta = 0.26$ (MR), and with $f_1 = 0.624$ and $\beta = 0.25$ (OS).

C. Continuous packings of irregularly shaped particles

Sohn and Moreland [25] measured the packing fraction of two sands with a lognormal size distribution. Systems of any desired mean size and standard deviation were synthesized by the addition of appropriate weights of closely sized fractions, obtained by sieving. Dense packings were obtained by tapping until no further volume reduction was observed. One sand ("MR") possessed a Wadell sphericity of about 0.81 and the other, more spherical, sand ("OS") a mean sphericity of 0.86. With the MR sand, for three different geometric mean sizes (viz. $d_g = 0.5$, 1, and 2 mm), the packing was measured for different standard variations (Fig. 6). One can see that the scatter among the three different means sizes is small, showing that the packing fraction is a function of the standard deviation only. For the OS the packing fraction was measured for different standard deviations, and here one geometric mean size only, namely $d_g = 0.3$ mm, was taken. Also these values are included in Fig. 6. With MR sand relatively large standard deviations were achieved ($\ln\sigma_g$ up to 1.4).

From the packing fraction values close to $\ln\sigma_g = 0$ one can conclude that the monosized packing fractions (f_1) of MR and OS are approximately 0.576 and 0.624, respectively. The higher sphericity of OS is reflected in its higher monosized packing fraction. The β of these sands is not known, but it can be conjectured that they lie between 0.2 (RCP of spheres) and 0.39 (RCP of distinctly angular particles), see Table III. In Fig. 6, Eq. (32) is drawn using the aforementioned values of f_1, and β equal to 0.25 and 0.26 for OS and MR, respectively. One can see that for all standard deviations, Eq. (32) is able to well predict the packing density in the entire $\ln\sigma_g$ range considered. In contrast to the sphere packings, β is now fitted as its value is unknown for the considered OS and MR sands. But it is seen that the β values correspond to the packing mode (RCP) and the sphericity of OS and MR sands, 0.25 and 0.26, respectively, and lie within the expected range, viz. between 0.2 and 0.39 (Table III).

V. CONCLUSIONS

In the present paper the void fraction of equally shaped polydisperse particles, with monosized void fraction φ_1 and having a lognormal size distribution, is addressed. First, the binary packing fraction of particle groups with large size ratio (noninteracting groups) and two different single packing fractions is considered for the entire compositional range. Subsequently, these equations are used to assess the packing fraction of n noninteracting size groups with a symmetrical binomial volume distribution. It appears that for large n, the void fraction asymptotically tends to $\varphi_1^{\sqrt{\pi n/2}}$, with φ_1 as the void fraction of one particle group. It appears that this expression is also accurate for $n \geq 2$ (Table II).

Next binomially distributed particles are considered, where each group consists of one particle size and subsequent particle sizes have a constant size ratio u. This ratio is reduced to unity, and the number of size groups is taken to be infinity. This limit yields a continuous lognormal size distribution. Taking this limit also yields a closed-form expression for the void fraction of this particle size distribution [Eq. (31)]. This void fraction depends on the monosized void fraction φ_1, the standard deviation $\ln\sigma_g$ of the distribution, and the contraction parameter β. This latter property governs the contraction that disordered packings undergo when a monosized distribution becomes a binary distribution of discretely sized particles (so near $u = 1$), governed by Eq. (29). Likewise, the unimodal void fraction, φ_1, β is a nonadjustable property that is governed by particle shape and mode of packing only. For a number of particle shapes and modes of packing its value is extracted from computer simulations and experiments and their values are summarized in Table III. The positive magnitude of β is a measure for the packing fraction increase (or void fraction decrease) when disordered monosized packings become polydisperse, as is the case with the continuous lognormal size distributions considered here and which was also seen with geometric (power-law) size distributions [23]. Furthermore, for RCP the β values of spheres and irregular particles range significantly (Table III). This difference in β is smaller among the different particle shapes when the particles are packed in loose state (as is also the case for the monosized packing fraction) [23,34]. On the other hand, for crystalline or ordered packings, β has a negative value, reflecting the expansion of these packing arrangements when the monosized situation is abandoned [36]. As Eqs. (16) and (29) also hold for ordered packings, Eq. (31) is also applicable when their particle sizes are lognormally distributed.

The obtained closed-form expressions for the packing or void fraction of lognormal size distributions is found to be in good quantitative agreement with experimental and computer-generated packing data. This comparison concerns RLP and RCP of spheres with a wide range of standard deviations. This agreement is achieved by using the known values of φ_1 and β, without the need of any adjustment. Also, for irregularly shapes particles, two sands with different angularities, good agreement is obtained in the entire standard deviation range. Here β was not known *a priori* and, hence, needed to be assessed, but their values are lying within the narrow range expected beforehand.

ACKNOWLEDGMENTS

The author wishes to thank Dr. P. Spiesz, Dr. G. Hüsken (BAM Federal Institute for Materials Research and Testing), and Dr. M. Hunger (HeidelbergCement Benelux) for their assistance with the retrieving of the computational and experimental data presented in Figs. 5 and 6.

APPENDIX

In this Appendix the derivation of the equations presented in Table I, for the case $n = 8$, is presented. These expressions concern the packing of monosized particles, with constant size ratio u, binomially distributed according to Eq. (10) with $p = ½$ as the distribution is symmetrical. The size ratio is such that all particle size classes are noninteracting, so $d_i/d_{i+1} = u > u_b$, and, hence, that Eqs. (8) and (9) are applicable.

As all size fractions are noninteracting, first only the two largest size fractions, with volume fractions $c_1 = 1/128$ and $c_2 = 7/128$, are combined, each having a packing fraction $\varphi_1 = \varphi_L = \varphi_S$, and a binary composition $c_L = 1/8$ and $c_S = 7/8$. Subsequently, Eq. (4) yields $c_L^{\text{sat}} = 1/(1 + \varphi_1)$ and as $0 \le \varphi_1 \le 1$, $c_L < c_L^{\text{sat}}$. Accordingly, curve A, i.e., Eq. (8), of Fig. 1 is applicable. Using Eq. (8) yields

$$\varphi_{12} = \frac{7\varphi_1}{8 - \varphi_1}, \tag{A1}$$

where φ_{12} reflects the void fraction of sizes 1 and 2 and which is used instead of symbol h from Eq. (8).

Next, this binary packing is combined with smaller size fraction 3, with volume fraction $c_3 = 21/128$ and void fraction $\varphi_S = \varphi_1$. The large fraction, combined sizes 1 and 2, have a volume fraction of $8/128$ $(= c_1 + c_2)$ and a void fraction $\varphi_L = 7\varphi_1/(8 - \varphi_1)$, see Eq. (A1). Equation (4) yields $c_L^{\text{sat}} = 8/(8 + 7\varphi_1)$. For this binary mix of c_3 on the one hand and $c_1 + c_2$ on the other, holds $c_L = 8/29$, and as $0 \le \varphi_1 \le 1$, $c_L < c_L^{\text{sat}}$. Accordingly, curve A, i.e., Eq. (8), of Fig. 1 is again applicable. Using Eq. (8) yields as a void fraction of the combined sizes 1, 2, and 3,

$$\varphi_{1-3} = \frac{21\varphi_1}{29 - 8\varphi_1}. \tag{A2}$$

The three size fractions are combined with size fractions 4 and 5. As an intermediate step, size fractions 4 and 5 are combined first, having volume fractions $c_4 = c_5 = 35/128$ and void fraction $\varphi_L = \varphi_S = \varphi_1$. Equation (4) yields $c_L^{\text{sat}} = 1/(1 + \varphi_1)$. For this binary mix, with composition $c_L = ½$ and considering $0 \le \varphi_1 \le 1$, $c_L \leqslant c_L^{\text{sat}}$ holds. Accordingly, curve A and Eq. (8) are applicable,

$$\varphi_{45} = \frac{\varphi_1}{2 - \varphi_1}, \tag{A3}$$

Now small sizes 4 and 5 are combined with larger sizes 1–3. Equation (4) with $\varphi_L = \varphi_{45}$ and $\varphi_S = \varphi_{1-3}$ yields $c_L^{\text{sat}} = 29(2 - \varphi_1)/(58-16\varphi_1)$, in which Eqs. (A2) and (A3) are substituted. The volume fraction of the large fraction c_L in the binary mix is $29/99$ (as $c_1 + c_2 + c_3 = 29/128$ and $c_4 + c_5 = 70/128$). It can readily be verified, as $0 \le \varphi_1 \le 1$, that $c_L = c_L^{\text{sat}}$, so curve A, described by Eq. (8), can be applied, yielding

$$\varphi_{1-5} = \frac{35\varphi_1}{99 - 64\varphi_1}. \tag{A4}$$

Equation (A4) gives the void fraction of combined size fractions 1 to 5.

Next, the two smallest fractions, 8 and 7, are combined with volume fractions $c_8 = 1/128$ and $c_7 = 7/128$, each having a packing fraction $\varphi_1 = \varphi_L = \varphi_S$, and a binary composition $c_L = 7/8$ and $c_S = 1/8$. Equation (4) yields $c_L^{\text{sat}} = 1/(1 + \varphi_1)$. Hence, for $\varphi_1 \le 1/7$ it follows that $c_L < c_L^{\text{sat}}$ and curve A and Eq. (8) hold, whereas for $\varphi_1 \ge 1/7$ holds $c_L \ge c_L^{\text{sat}}$ and, consequently, curve B and Eq. (9) are applicable,

$$\varphi_{78} = \frac{\varphi_1}{8 - 7\varphi_1} \quad (0 \leqslant \varphi_1 \leqslant 1/7), \tag{A5}$$

$$\varphi_{78} = \frac{8\varphi_1 - 1}{7} \quad (1/7 \leqslant \varphi_1 \leqslant 1), \tag{A6}$$

whereby $c_L = 7/8$ and $\varphi_L = \varphi_S = \varphi_1$ are used.

These two combined fraction are combined with fraction 6, with volume fraction $c_6 = 21/128$ and void fraction $\varphi_L = \varphi_1$. The small fraction, consisting of sizes 7 and 8, has a volume fraction of $8/128$ $(= c_7 + c_8)$, and their void fraction, $\varphi_S = \varphi_{78}$, depends on φ_1 and is given by Eqs. (A5) and (A6). For this binary mix, of c_6 on the one hand and $c_7 + c_8$ on the other, holds $c_L = 21/29$.

First, the case $0 \le \varphi_1 \le 1/7$ is examined. Equation (4), with $\varphi_L = \varphi_1$ and $\varphi_S = \varphi_{78}$ [Eq. (A5)], yields $c_L^{\text{sat}} = (8 - 7\varphi_1)/(8 + \varphi_1)$. For $0 \le \varphi_1 \le 1/7$ it follows that $c_L < c_L^{\text{sat}}$, so Eq. (8) applies as follows:

$$\varphi_{6-8} = \frac{\varphi_1}{29 - 28\varphi_1} \quad (0 \leqslant \varphi_1 \leqslant 1/7), \tag{A7}$$

where $c_L = 21/29$ and $\varphi_S = \varphi_{78}$ [Eq. (A5)] are substituted. Second, the case $(1/7 \le \varphi_1 \le 1)$ is considered. Equation (4), with $\varphi_L = \varphi_1$ and $\varphi_S = \varphi_{78}$ [Eq. (A6)], yields $c_L^{\text{sat}} = 7/(7 + 8\varphi_1)$. Hence, for $1/7 \le \varphi_1 \le 1/3$ it follows that $c_L < c_L^{\text{sat}}$ and curve A and Eq. (8) hold, whereas for $1/3 \le \varphi_1 \le 1$, $c_L \ge c_L^{\text{sat}}$ holds and, consequently, curve B and Eq. (9) are applicable as follows:

$$\varphi_{6-8} = \frac{8\varphi_1 - 1}{28 - 21\varphi_1} \quad (1/7 \leqslant \varphi_1 \leqslant 1/3), \tag{A8}$$

$$\varphi_{6-8} = \frac{29\varphi_1 - 8}{21} \quad (1/3 \leqslant \varphi_1 \leqslant 1), \tag{A9}$$

where $c_L = 21/29$, $\varphi_L = \varphi_1$, and $\varphi_S = \varphi_{78}$ [Eq. (A6)] are substituted.

Finally, all eight size fractions are combined, the five largest sizes with total volume fraction $c_L = 99/128$ $(= c_1 + \cdots + c_5)$ and their void fraction governed by Eq. (A4) and the three smallest sizes with total volume fraction $c_S = 29/128$ $(= c_6 + c_7 + c_8)$ and their void fraction governed by Eqs. (A7)–(A9).

First, the case $0 \le \varphi_1 \le 1/7$ is addressed. Equation (4), with $\varphi_L = \varphi_{1-5}$ [Eq. (A4)] and $\varphi_S = \varphi_{6-8}$ [Eq. (A7)], yields $c_L^{\text{sat}} = (29 - 28\varphi_1)/(2871 - 1757\varphi_1)$. For $0 \le \varphi_1 \le 1/7$ it

follows that $c_L = 99/128 < c_L^{\rm sat}$, so Eq. (8) applies,

$$\varphi_8^{\rm BN} = \frac{\varphi_1}{128 - 127\varphi_1} \quad (0 \leqslant \varphi_1 \leqslant 1/7). \tag{A10}$$

This is the void fraction of a packing with a binomial size distribution in the given range of the single component void fraction φ_1. Next the case $1/7 \leq \varphi_1 \leq 1/3$ is considered. Equation (4), with $\varphi_L = \varphi_{1-5}$ [Eq. (A4)] and $\varphi_S = \varphi_{6-8}$ [Eq. (A8)], yields $c_L^{\rm sat} = 99(28 - 21\varphi_1)/(2772 - 1064\varphi_1)$. For $1/7 \leq \varphi_1 \leq 1/3$ it follows that $c_L = 99/128 < c_L^{\rm sat}$, so Eq. (8) applies as follows:

$$\varphi_8^{\rm BN} = \frac{8\varphi_1 - 1}{127 - 120\varphi_1} \quad (1/7 \leqslant \varphi_1 \leqslant 1/3). \tag{A11}$$

For the case $1/3 \leq \varphi_1 \leq 1$, Eq. (4), with $\varphi_L = \varphi_{1-5}$ [Eq. (A4)] and $\varphi_S = \varphi_{6-8}$ [Eq. (A9)], yields $c_L^{\rm sat} = 297/(297 + 145\varphi_1)$. Hence, for $1/3 \leq \varphi_1 \leq 3/5$ it follows that $c_L < c_L^{\rm sat}$ and curve A and Eq. (8) hold, whereas for $3/5 \leq \varphi_1 \leq 1$, $c_L \geq c_L^{\rm sat}$ holds and, consequently, curve B and Eq. (9) are applicable as follows:

$$\varphi_8^{\rm BN} = \frac{29\varphi_1 - 8}{120 - 99\varphi_1} \quad (1/3 \leqslant \varphi_1 \leqslant 3/5), \tag{A12}$$

$$\varphi_8^{\rm BN} = \frac{64\varphi_1 - 29}{99 - 64\varphi_1} \quad (3/5 \leqslant \varphi_1 = 1), \tag{A13}$$

where $c_L = 99/128$ and φ_L and φ_S follow from Eqs. (A4) and (A9), respectively. Equations (A10)–(A13) govern the void fraction of particle packings consisting of eight binomially distributed and noninteracting sizes, where each individual fraction has a void fraction φ_1. The expressions depend on the magnitude of φ_1, and the four expressions are included in Table I.

[1] J. Aitchison and J. A. C. Brown, *The Log-Normal Distribution* (Cambridge University Press, Cambridge, 1957).
[2] J. H. Gaddum, Nature **156**, 463 (1945).
[3] S. C. Pearce, Nature **156**, 747 (1945).
[4] E. Limpert, W. A. Stahel, and M. Abbt, BioSci. **53**, 341 (2001).
[5] A. N. Kolmogoroff, Comptes rendu (Doklady) de l'Académie des Sciences de l'USSR **31**, 99 (1941) [in German].
[6] C. G. Granqvist and R. A. Buhrman, J. Appl. Phys. **47**, 2200 (1976).
[7] J. Söderlund, L. B. Kiss, G. A. Niklasson, and C. G. Granqvist, Phys. Rev. Lett. **80**, 2386 (1998); L. B. Kiss, J. Söderlund, G. A. Niklasson, and C. G. Granqvist, Nano Struct. Mat. **12**, 327 (1999).
[8] G. D. Scott, Nature **188**, 908 (1960); G. D. Scott and D. M. Kilgour, J. Phys. D: Appl. Phys. **2**, 863 (1969).
[9] A. S. Clarke and J. D. Wiley, Phys. Rev. B **35**, 7350 (1987).
[10] A. P. Shapiro and R. F. Probstein, Phys. Rev. Lett. **68**, 1422 (1992).
[11] A. Yang, C. T. Miller, and L. D. Turcoliver, Phys. Rev. E **53**, 1516 (1996).
[12] D. He, N. N. Ekere, and L. Cai, Phys. Rev. E **60**, 7098 (1999).
[13] A. R. Kansal, S. Torquato, and F. H. Stillinger, J. Chem. Phys. **117**, 8212 (2002); Phys. Rev. E **66**, 041109 (2002).
[14] G. W. Delaney, T. Di Matteo, and T. Aste, Soft Matter **6**, 2992 (2010).
[15] G. Y. Onoda and E. G. Liniger, Phys. Rev. Lett. **64**, 2727 (1990).
[16] T. Aste, M. Saadatfar, and T. J. Senden, J. Stat. Mech. (2006) P07010.
[17] M. Jerkins, M. Schröter, H. L. Swinney, T. J. Senden, M. Saadatfar, and T. Aste, Phys. Rev. Lett. **101**, 018301 (2008).
[18] C. Song, P. Wang, and H. A. Makse, Nature **453**, 629 (2008).
[19] J. G. Berryman, Phys. Rev. A **27**, 1053 (1983).
[20] A. P. Philipse, Langmuir **12**, 1127 (1996); **12**, 5971 (1996).
[21] W. Man, A. Donev, F. H. Stillinger, M. T. Sullivan, W. B. Russel, D. Heeger, S. Inati, S. Torquato, and P. M. Chaikin, Phys. Rev. Lett. **94**, 198001 (2005).
[22] C. C. Furnas, Ind. Eng. Chem. **23**, 1052 (1931).
[23] H. J. H. Brouwers, Phys. Rev. E **74**, 031309 (2006); **74**, 069901(E) (2006); **84**, 059905(E) (2011).
[24] H. J. H. Brouwers, Phys. Rev. E **84**, 042301 (2011).
[25] H. Y. Sohn and C. Moreland, Can. J. Chem. Eng. **46**, 162 (1968).
[26] A. R. Dexter and D. W. Tanner, Nature **238**, 31 (1972).
[27] C. C. Furnas, Department of Commerce, Bureau of Mines, Report of Investigation Serial No. 2894, 1928; Bull. U.S. Bureau Mines **307**, 74 (1929).
[28] R. K. McGeary, J. Am. Ceram. Soc. **44**, 513 (1961).
[29] M. A. Caquot, Mémoires de la Société des Ingénieurs Civils de France, 562 (in French) (1937).
[30] R. S. Farr and R. D. Groot, J. Chem. Phys. **131**, 244104 (2009).
[31] A. V. Kyrylyuk, A. Wouterse and A. P. Philipse, Prog. Colloid Polym. Sci. **137**, 29 (2010).
[32] A. B. Hopkins, F. H. Stillinger, and S. Torquato, Phys. Rev. E **88**, 022205 (2013).
[33] Their binary packing fraction of unimodal spheres is expressed in the number fraction x of the small component [Eq. (B4)], reading $\Phi_{\rm MRJ} = a\,(1 - x + x\alpha^3)/[1 - x + x\alpha^3(1 - h)]$ with $h = 0.934$ for $\alpha = u^{-1} = 0.2$. Considering that η corresponds to $\Phi_{\rm MRJ}$, $f_L\,(= f_S = f_1)$ to a, and $c_S = 1 - c_L = x\alpha^3/(1 - x + x\alpha^3)$, η in Eq. (9) yields $\Phi_{\rm MRJ} = a\,(1 - x + x\alpha^3)/(1 - x)$, implying $h = 1$. It is also noteworthy to point out that, expressed in the volume fraction, $c_S^{\rm sat}$ reads $\varphi_1/(1 + \varphi_1)$ according to Eq. (4), and in the number fraction the saturation composition reads $x^{\rm sat} = \varphi_1/(\alpha^3 + \varphi_1)$, so tending to unity as α tends to zero.
[34] T. Koshy, *Catalan Numbers with Applications* (Oxford University Press, Oxford, 2009).
[35] W. Feller, *An Introduction to Probability Theory and Its Applications*, Vol. I, 3rd ed. (John Wiley, New York, 1970).
[36] H. J. H. Brouwers, Phys. Rev. E **87**, 032202 (2013).
[37] M. Hunger, PhD thesis, Eindhoven University of Technology, Eindhoven, 2010; Private communications (2013).
[38] R. Jeschar, W. Pötke, V. Petersen, and K. Polthier, *Proceedings Symposium on Blast Furnace Aerodynamics, Wollongong, Australia, 25th–27th September 1975*, edited by N. Standish, pp. 136–147, Illawara Branch of the Australasian Institute of Mining and Metallurgy (Aus. I.M.M., Carlton, Australia, 1975).
[39] M. J. Powell, Powder Technol. **25**, 45 (1980).
[40] M. Suzuki and T. Oshima, Powder Technol. **35**, 159 (1983); **44**, 213 (1985).